Supporting Information

Ultrathin Microporous Metal-Organic Network Membranes for Molecular Separation

Shenxiang Zhang[a,b], *Richard Ciora*[b,c], *Bratin Sengupta*[b,c], *Huazheng Li*[b,c], *Georges Belfort*[b], *Shiguang Li*[d], *Rongfei Zhou*[e], *and Miao Yu**[b,c]

[a]College of Chemistry, Chemical Engineering and Materials Science, Soochow University, Suzhou 215123, P.R. China.

[b] Department of Chemical and Biological Engineering, Rensselaer Polytechnic Institute, Troy, NY 12180, USA.

[c]Department of Chemical and Biological Engineering and RENEW Institute, University at Buffalo, Buffalo, NY 14260, USA.

[d]Gas Technology Institute, 1700 South Mount Prospect Road, Des Plaines, IL 60018, USA.

[e]State Key Laboratory of Materials-Oriented Chemical Engineering, College of Chemical Engineering, Nanjing Tech University, Nanjing 210009, P. R. China

*Correspondence to: myu9@buffalo.edu

Supplementary Figures

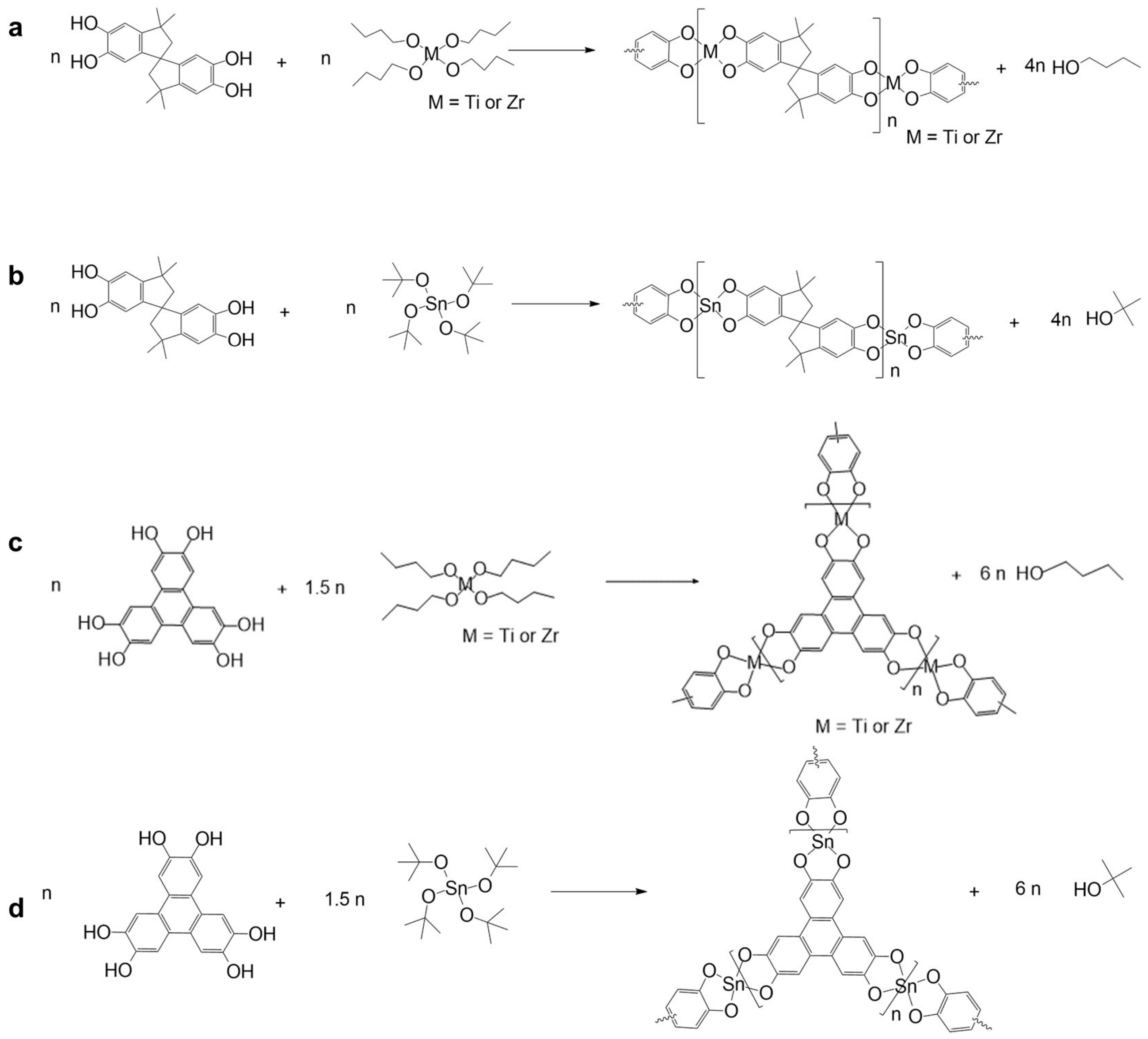

Fig. S1 Proposed reaction scheme of (**a**) TTSBI-Ti/Zr, (**b**) TTSBI-Sn, (**c**) HHTP-Ti/Zr, and (**d**) HHTP-Sn.

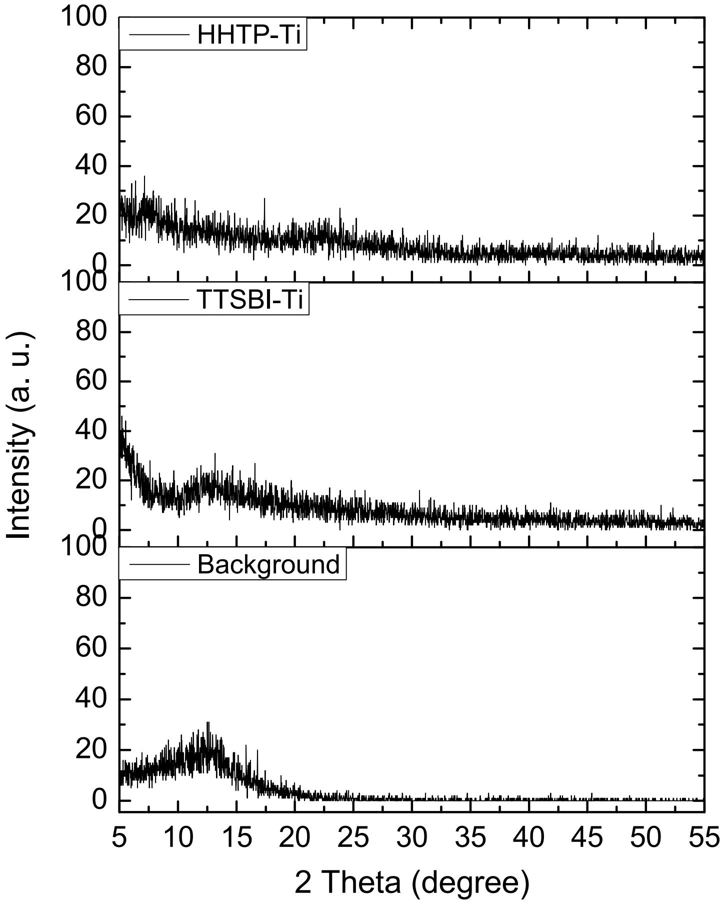

Fig. S2 XRD patterns of TTSBI-Ti and HHTP-Ti particles.

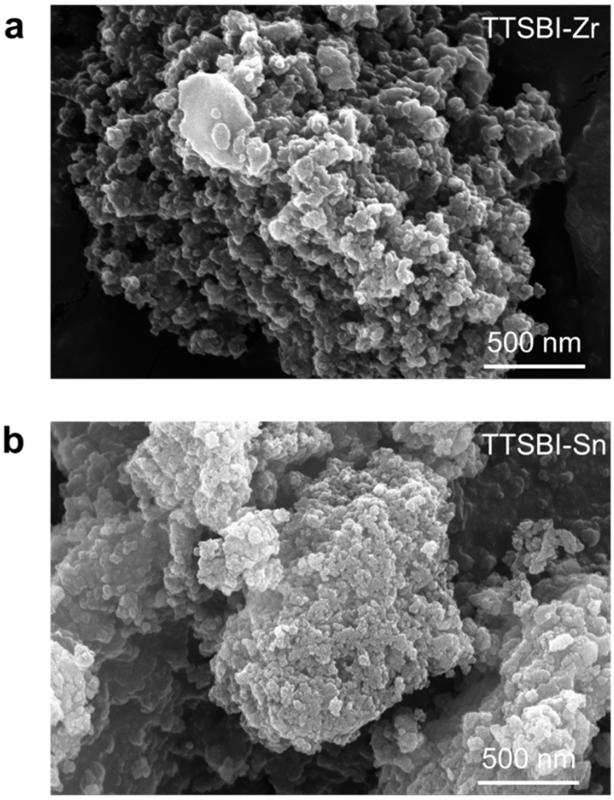

Fig. S3 SEM images of (**a**) TTSBI-Zr and (**b**) TTSBI-Sn particles.

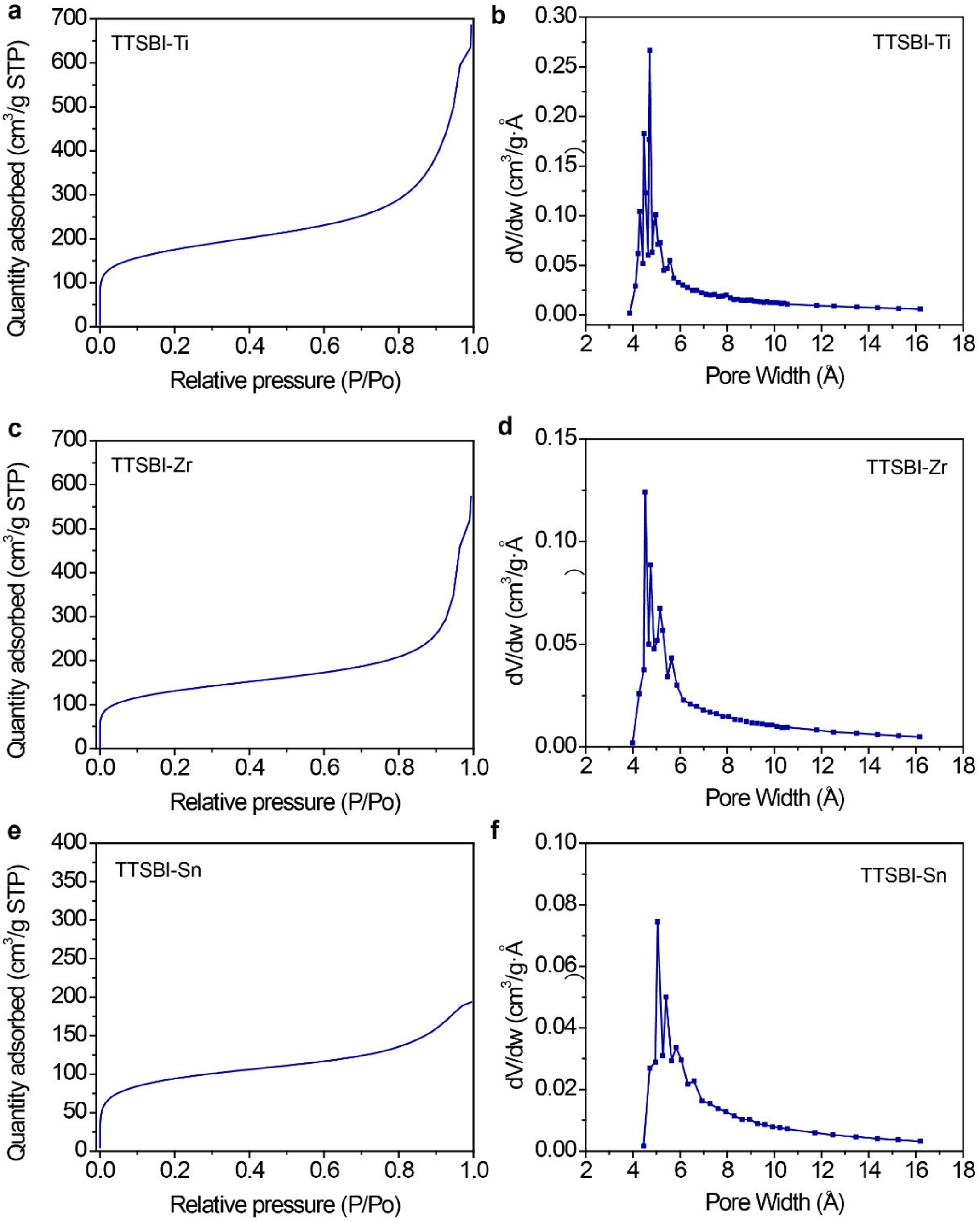

Fig. S4 (**a**, **c** and **e**) N_2 adsorption isotherms at 77 K and (**b**, **d** and **f**) pore size distribution for (**a**, **b**) TTSBI-Ti, (**c**, **d**) TTSBI-Zr, (**e**, **f**) TTSBI-Sn particles.

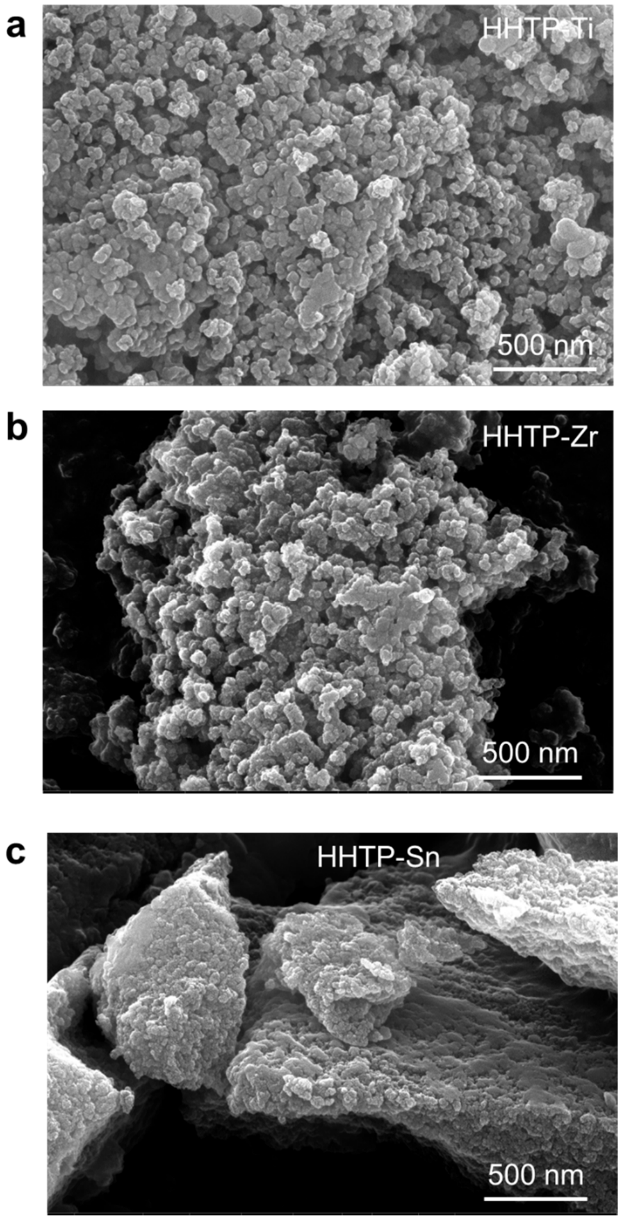

Fig. S5 SEM images of (**a**) HHTP-Ti, (**b**) HHTP-Zr and (**c**) HHTP-Sn particles.

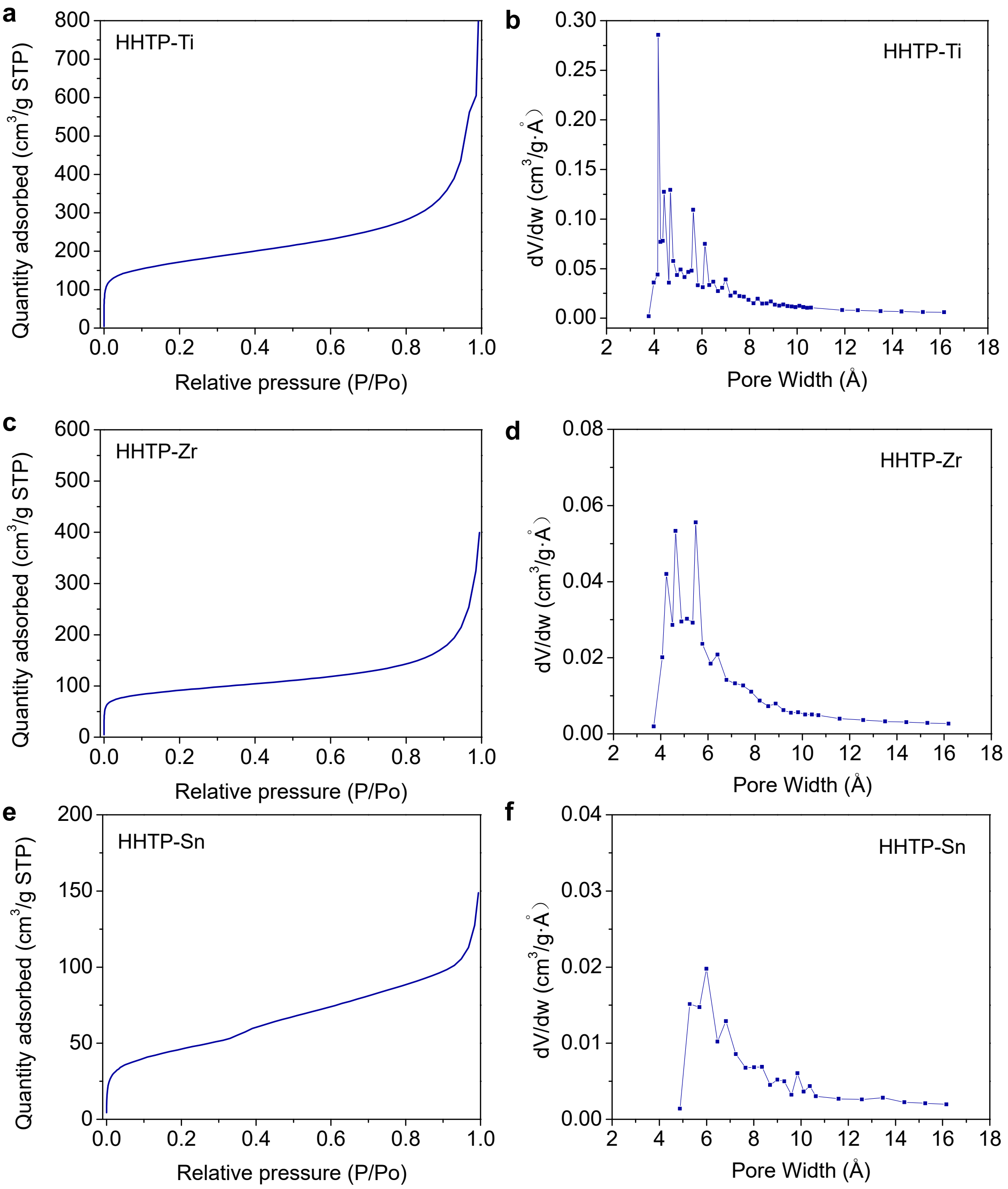

Fig. S6 (**a**, **c** and **e**) N_2 adsorption isotherms at 77 K and (**b**, **d** and **f**) pore size distribution for (**a**, **b**) HHTP-Ti, (**c**, **d**) HHTP-Zr, (**e**, **f**) HHTP-Sn particles.

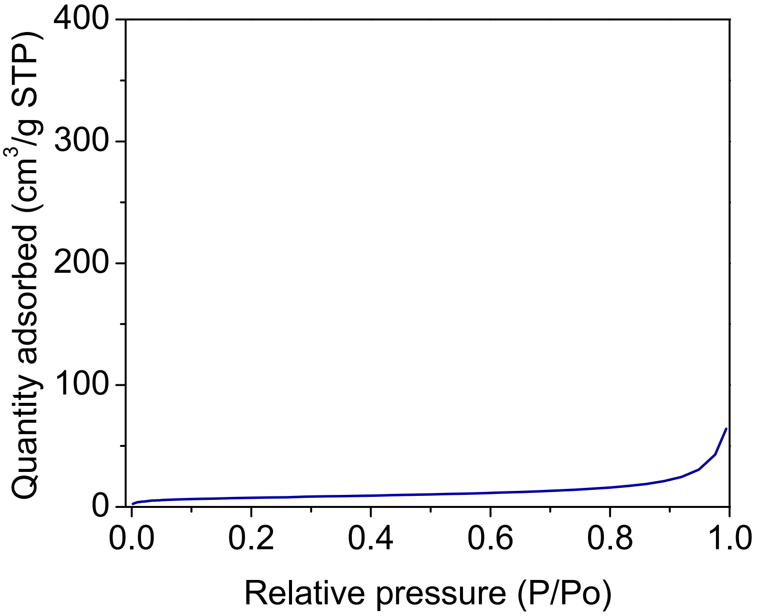

Fig. S7 N_2 adsorption isotherms at 77 K for EG-Ti particles. EG-Ti particles were prepared by using $TiCl_4$ and ethylene glycol (EG) as precursors. 0.2 mL $TiCl_4$ was quickly added into 5.0 mL EG solution with continuous stirring at room temperature. After 10-min reaction, the white precipitate was collected by centrifuge, and then washed by acetone for 3 times. It was subsequently dried in a vacuum oven at 90 °C for 12 h.

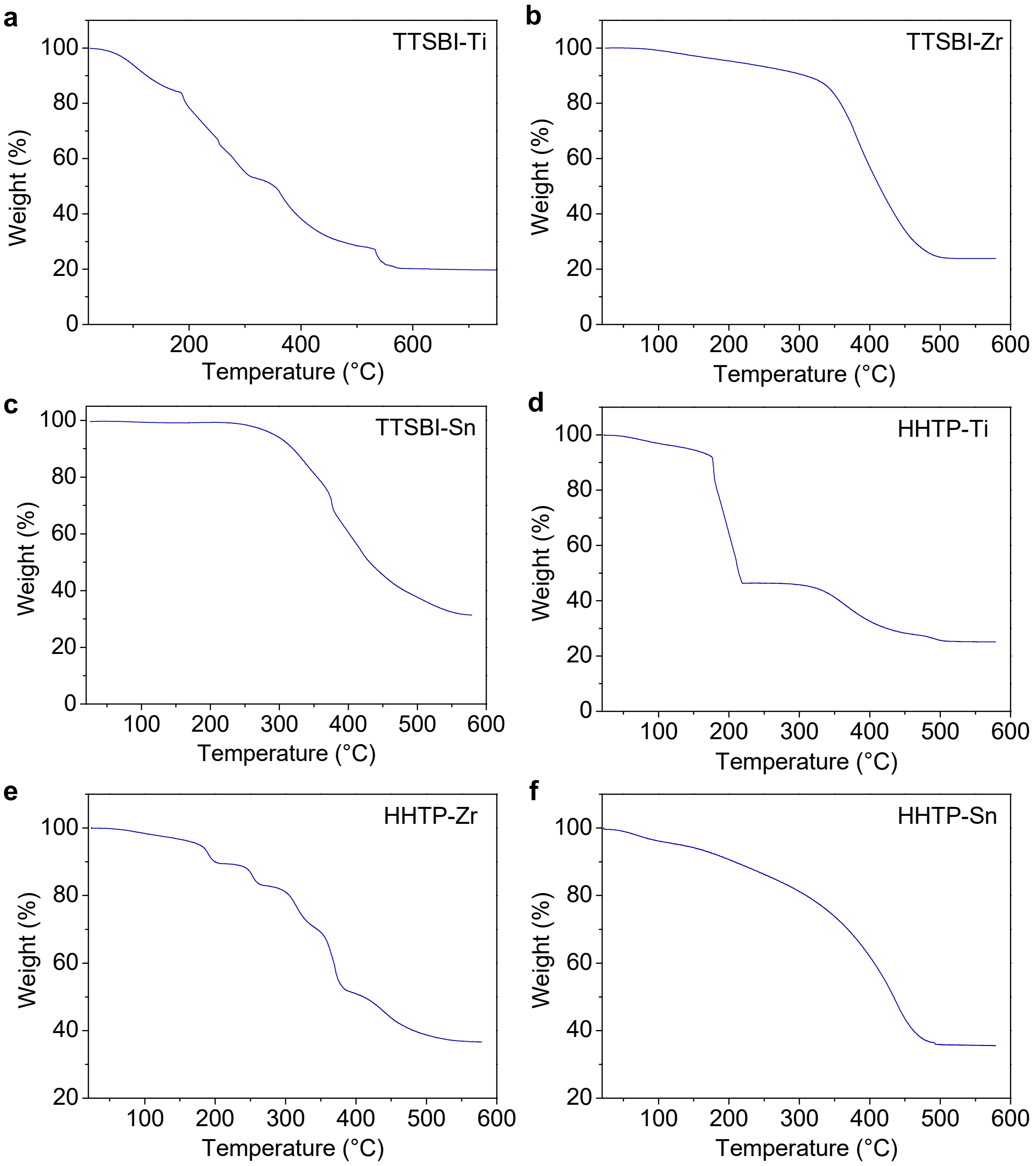

Fig. S8 Thermogravimetric analysis of (**a**) TTSBI-Ti, (**b**) TTSBI-Zr, (**c**) TTSBI-Sn, (**d**) HHTP-Ti, (**e**) HHTP-Zr, and (**f**) HHTP-Sn particles in air atmosphere. Heating rate: 10 °C/min.

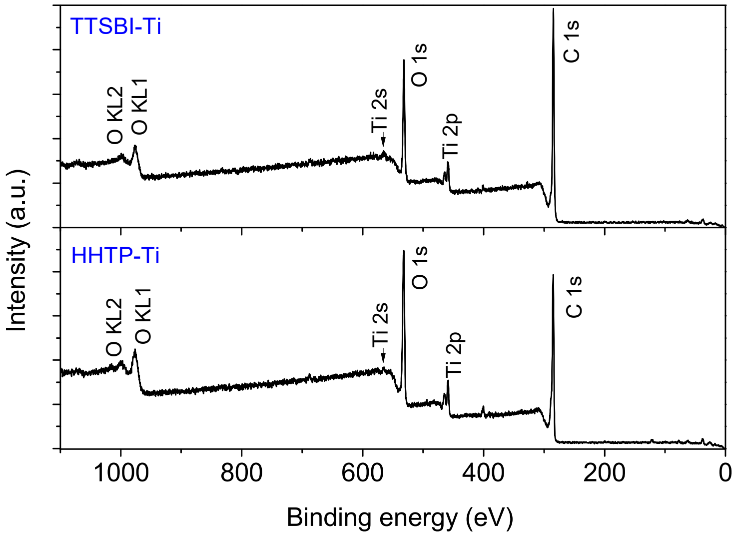

Fig. S9 XPS survey spectra of TTSBI-Ti and HHTP-Ti particles.

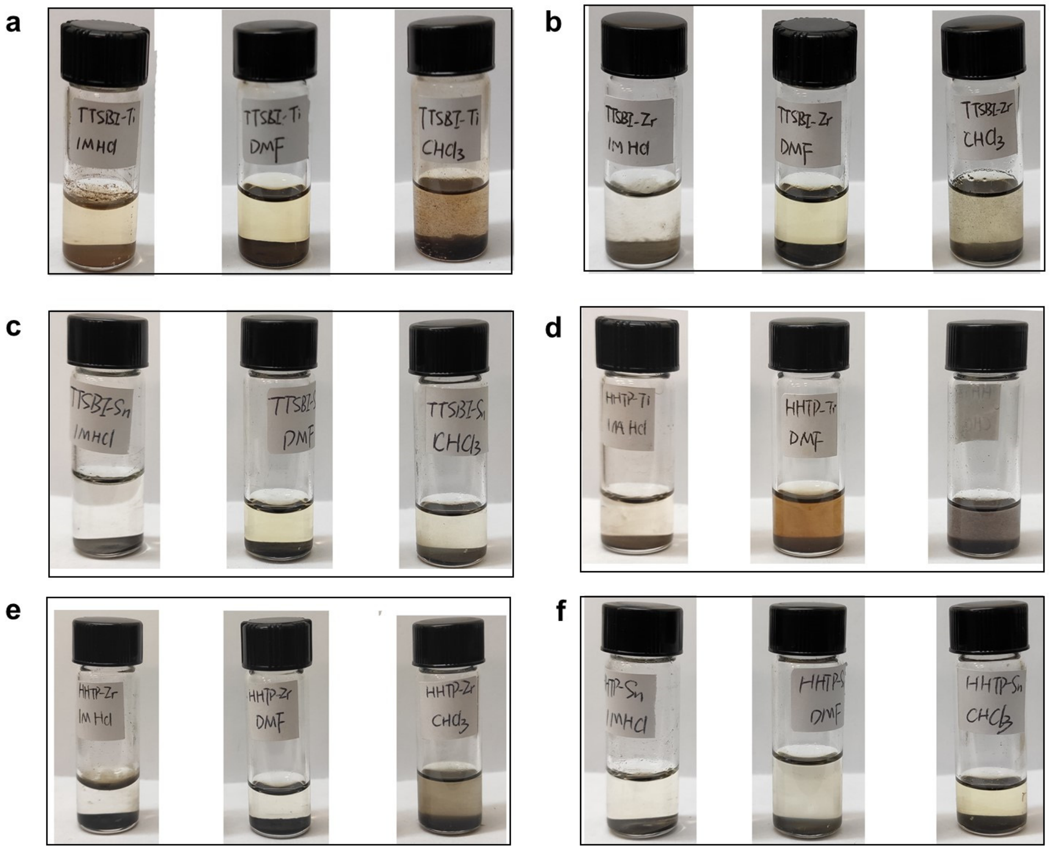

Fig. S10 Photographs of (**a**) TTSBI-Ti, (**b**) TTSBI-Zr, (**c**) TTSBI-Sn, (**d**) HHTP-Ti, (**e**) HHTP-Zr and (**f**) HHTP-Sn particles in 1 M HCl, N-methyl-2-pyrrolidone (NMP) and chloroform (from left to right) after being soaked for 3 days.

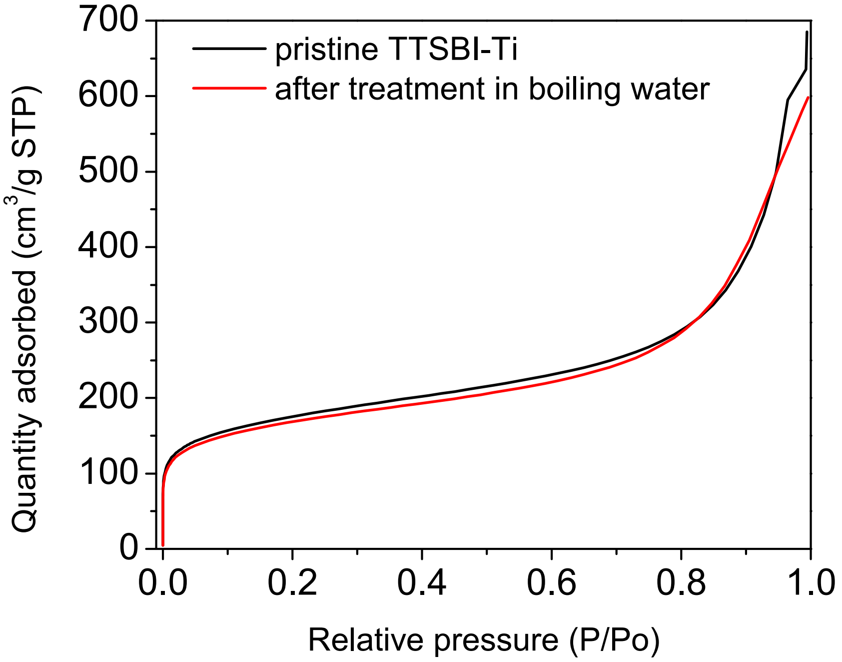

Fig. S11 N_2 adsorption isotherms at 77 K for TTSBI-Ti particles before and after being soaked in boiling water for 1 day.

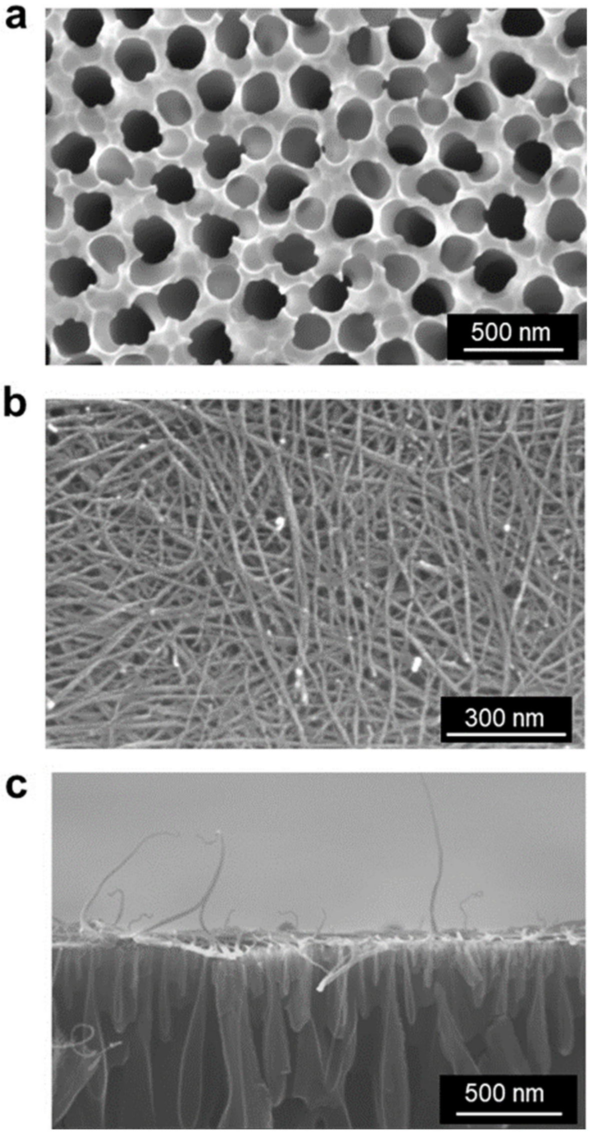

Fig. S12 (**a**) Surface SEM image of bare AAO support. (**b**) Surface SEM image of CNT network. (**c**) Cross-section SEM image of CNT network with thickness of ~90 nm on AAO support.

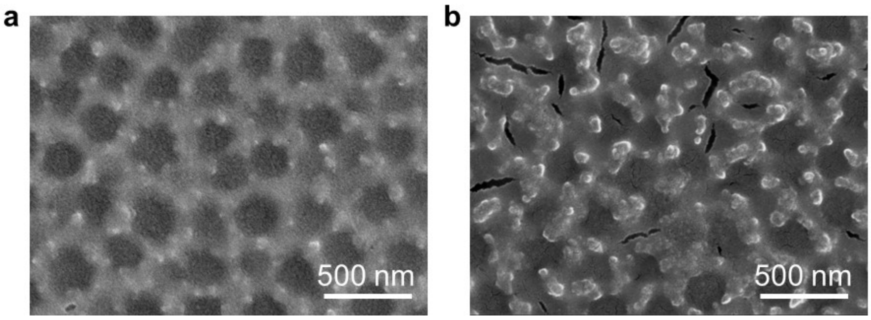

Fig. S13. SEM images of TTSBI-Ti 60-nm membrane on AAO substrate without using CNT network as interlayer: (a) before OSN performance test and (b) after OSN performance test with 5 bar transmembrane pressure drop.

A control experiment was also carried out in this work. The AAO (pore size: 150-200 nm) supported TTSBI-Ti membrane was synthesized by interfacial reaction without using CNT network as the interlayer. As shown in Fig. S13a below, a thin and continuous TTSBI-Ti membrane can be observed on the surface of the AAO substrate. However, the mechanical strength of TTSBI-Ti selective layer (with the thickness of only 60 nm) was not strong enough to withstand 5 bar transmembrane pressure drop during separation testing. Fig. S13b below shows that obvious cracks can be seen in the TTSBI-Ti selective layer after OSN performance test. We also tried to synthesize TTSBI-Ti membrane on AAO substrate with smaller pore size of ~20 nm. This issue could be resolved. But the methanol permeance decreased to <2 L m^{-2} h^{-1} bar^{-1}, owing to the lower surface porosity on 20 nm pore size AAO substrate than 200 nm pore size AAO substrate.

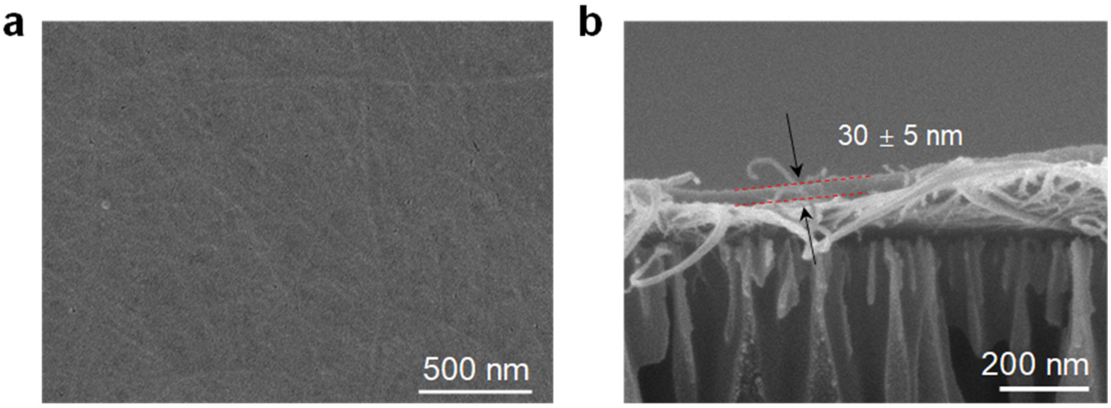

Fig. S14 (**a**) Surface and (**b**) cross-sectional SEM images of HHTP-Ti membrane prepared by interfacial reaction of $Ti(OBu)_4$ (10 mM) in tetradecane and HHTP (20 mM) in NMP.

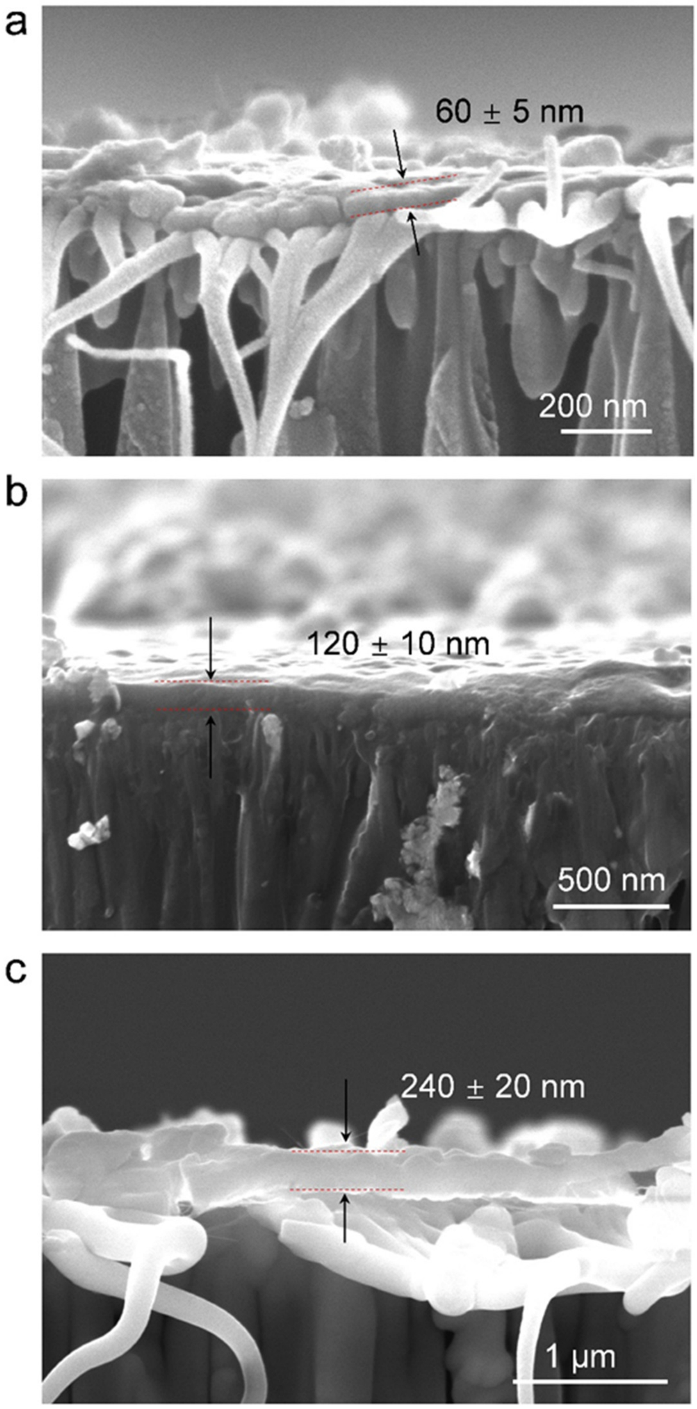

Fig. S15 Interfacial synthesis of TTSBI-Ti membrane with different thicknesses. **a**, Cross-sectional SEM image of TTSBI-Ti membrane prepared by interfacial reaction of $Ti(OBu)_4$ (20 mM) in tetradecane and TTSBI (40 mM) in NMP. **b**, Cross-sectional SEM image of TTSBI-Ti membrane prepared by interfacial reaction of $Ti(OBu)_4$ (40 mM) in tetradecane and TTSBI (80 mM) in NMP. **c**, Cross-sectional SEM image of TTSBI-Ti membrane prepared by interfacial reaction of $Ti(OBu)_4$ (80 mM) in tetradecane and TTSBI (160 mM) in NMP.

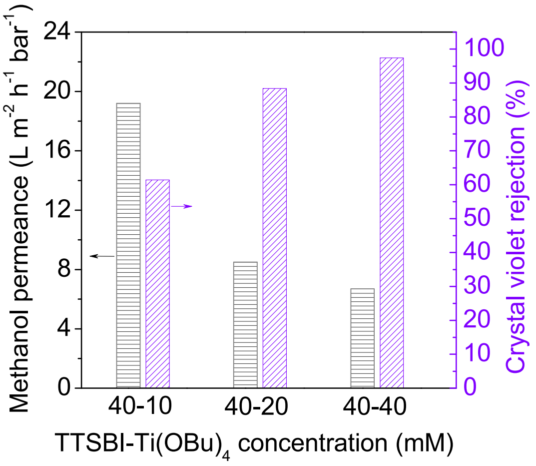

Fig. S16 Methanol permeance and CV rejection of the TTSBI-Ti membranes prepared by interfacial reaction between TTSBI (40 mM in NMP) and Ti(OBu)$_4$ (10, 20 and 40 mM in tetradecane, respectively).

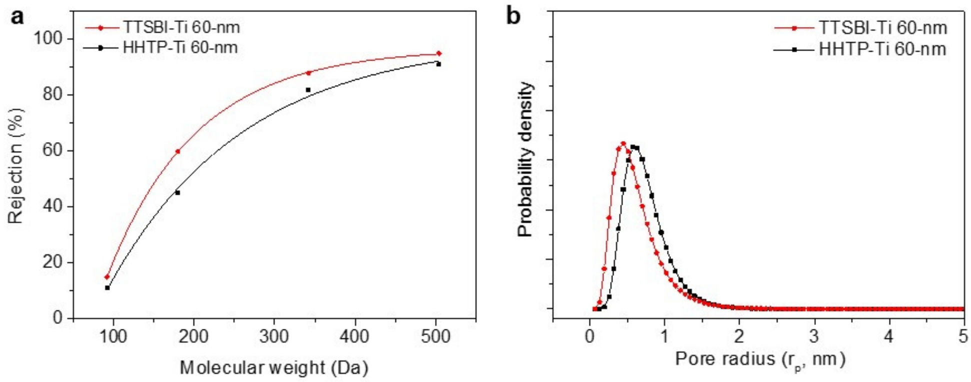

Fig. S17. (a) Rejection of uncharged model solutes including raffinose, sucrose, glucose, and glycerol by TTSBI-Ti 60-nm and HHTP-Ti 60-nm membranes. (b) Pore size distribution of TTSBI-Ti 60-nm and HHTP-Ti 60-nm membranes derived from rejection curves of uncharged solutes.

The pore size and pore size distribution of TTSBI-Ti 60-nm and HHTP-Ti 60-nm membranes were determined by the rejection of a series of neutral organic compounds, such as glycerol (92 Da, Stokes radii 0.26 nm), glucose (180 Da, Stokes radii 0.36 nm), sucrose (342 Da, Stokes radii 0.46 nm) and raffinose (504 Da, Stokes radii 0.54 nm). The concentration of each organic species solution was 200 ppm, and the applied pressure drop in the filtration experiments was 5 bar. The rejection results were presented in Fig. S17a. The pore size distribution curve is expressed as a probability density function (Equation 1) that was established based on the following assumption: (1) There is no steric or hydrodynamic interaction between these organic solutes and the membrane pores; (2) The mean pore radius of the TTSBI membrane equals the Stokes radius of the organic solute with a measured rejection of 50%; (3) The distribution of the membrane pore radius is characterized by the geometric standard deviation of the PDF curve, which is the ratio between the Stokes radius with a rejection of 84.13% to that with a rejection of 50% (*Nat. Commun.* **2020**, *11*, 2015; *RSC Adv.* **2015**, *5*, 40742).

$$\frac{dR(r_{\mathrm{p}})}{dr_{\mathrm{p}}} = \frac{1}{r_{\mathrm{p}} ln\sigma_{\mathrm{p}}\sqrt{2\pi}} \exp\left[-\frac{(lnr_{\mathrm{p}} - ln\mu_{\mathrm{p}})^2}{2(ln\sigma_{\mathrm{p}})^2}\right] \tag{1}$$

Where μ_{p} is the mean pore size, σ_{p} is the geometric standard deviation of the PDF curve, and r_{p} is the Stokes radius of the organic solute

As shown in Fig. S17b, TTSBI-Ti 60-nm membrane had a mean pore radius of 0.46 nm. HHTP-Ti 60-nm membrane had a mean pore radius of 0.59 nm, larger than TTSBI-Ti 60-nm. Both membranes showed a relatively broad pore size distribution.

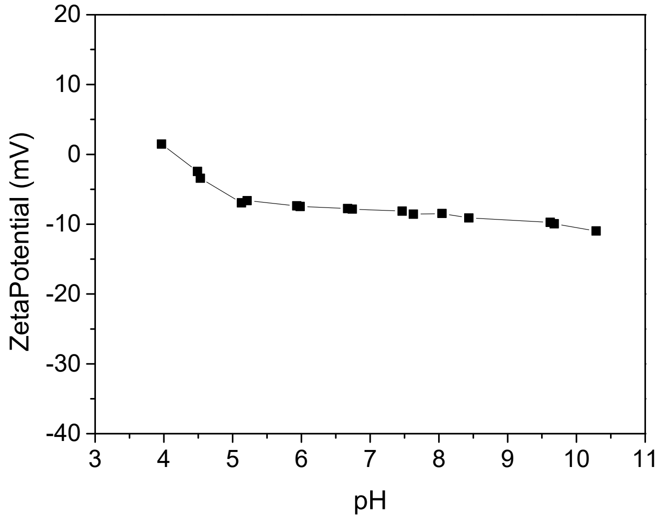

Fig. S18 Surface streaming potential of TTSBI-Ti membranes. The surface charge property of the membranes was investigated via zeta potential measurement. As shown Fig. S18, at pH value of 10 ~ 5, the TTSBI-Ti membrane exhibited a stationary zeta potential in the range of -9.6 ~ -6.9 mV and only a slight increase to 1.4 mV at pH = 4. Because there are no charged groups on the surface, TTSBI-Ti membrane showed nearly neutral characteristic.

Tab. S1 Surface area and pore volume of TTSBI-Ti particles before and after being soaked in boiling water, acid solutions, and DMF solvent.

Sample	**Treatment method**	**Time**	**BET surface area (m^2/g)**	**Micropore volume (cm^3/g)**
TTSBI-Ti	None		582	0.265
TTSBI-Ti	Soaked in boiling water at atmospheric pressure	1 day	557	0.255
TTSBI-Ti	Soaked in 1 M HCl solution	3 days	537	0.252
TTSBI-Ti	Soaked in DMF solvent	3 days	584	0.271

Tab. S2 Properties and structure of dyes used in OSN and molecular separation performance test.

Name	Structure	MW (g mol^{-1})
Azobenzene (AZ)	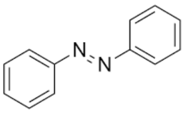	180.2
Methyl orange (MO)	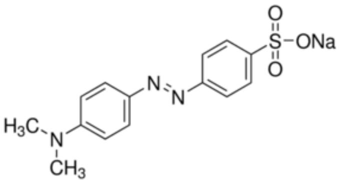	327.3
Crystal violet (CV)	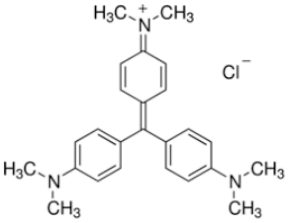	408.0
Indigo carmine (IC)	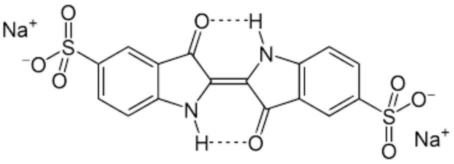	466.4
Brilliant blue R (BB)	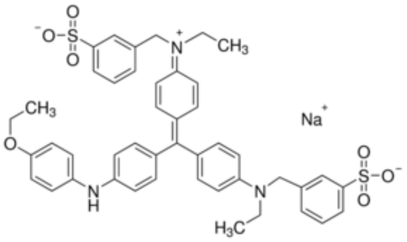	826.0

Tab. S3 Performance comparison with reported membranes.

	Membrane material	**Methanol permeance ($\mathrm{L\ m^{-2}\ h^{-1}\ bar^{-1}}$)**	**CV rejection (%)**	**Ref.**
1	PA/PSf	2	90	[1]
2	Polyetheramide	1.5	30	[2]
3	PAR-BHPF/PI	8.0	96	[3]
4	PAR-TTSBI/PI	6.0	98	[3]
5	PAR-DHAQ/PI	0.6	97	[3]
6	PAR-RES/PI	0.6	99	[3]
7	Highly laminated graphene oxide membranes	6.5	98	[4]
8	TiO_2+PA/PI mixed matrix membrane	26	90	[5]
9	TTSBI-Ti 60 nm	8.5	90	This work
10	HHTP-Ti 60 nm	12.5	58	This work

Supplementary references

[1] M. Peyravi, A. Rahimpour, M. Jahanshahi, *Journal of membrane science* **2012**, *423*, 225.

[2] M. M. A. Almijbilee, X. Wu, A. Zhou, X. Zheng, X. Cao, W. Li, *Separation and Purification Technology* **2020**, *234*, 116033.

[3] M. F. Jimenez-Solomon, Q. Song, K. E. Jelfs, M. Munoz-Ibanez, A. G. Livingston, *Nature materials* **2016**, *15*, 760.

[4] Q. Yang, Y. Su, C. Chi, C. Cherian, K. Huang, V. Kravets, F. Wang, J. Zhang, A. Pratt, A. Grigorenko, *Nature materials* **2017**, *16*, 1198.

[5] M. Peyravi, M. Jahanshahi, A. Rahimpour, A. Javadi, S. Hajavi, *Chemical Engineering Journal* **2014**, *241*, 155.